JOC The Journal of Organic Chemistry

Featured Article

pubs.acs.org/joc

Computational Elucidation of the Internal Oxidant-Controlled Reaction Pathways in Rh(III)-Catalyzed Aromatic C−H Functionalization

Liang Xu, Qi Zhu, Genping Huang, Bing Cheng, and Yuanzhi Xia*

College of Chemistry and Materials Engineering, Wenzhou University, Wenzhou 325035, P. R. China

Supporting Information

ABSTRACT: The Rh(III)-catalyzed C−H functionalizations of benzamide derivatives with olefin were studied by DFT calculations to elucidate the divergent pathways controlled by the *N*-OR internal oxidants. For substrates of *N*-OMe and *N*-OPiv internal oxidants, the energy profiles for consecutive N−H deprotonation/C−H activation/olefin insertion sequences were similar, and different properties and reactivities of the generated 7-membered rhodacycles were predicted. When *N*-OMe is involved, this intermediate is generally unstable, and the olefination occurs easily via a *β*-H elimination/reductive elimination (RE) sequence to generate the Rh(I) intermediate, which is then oxidized to the active Rh(III) via MeOH elimination from the *N*-OMe reduction in the presence of a HOAc. However, for a 7-membered rhodacycle containing a *N*-OPiv moiety, the coordination of the acyloxy carbonyl oxygen stabilizes this intermediate and increases the barrier of the olefination pathway. Instead, the migration of the acyloxy from N to Rh(III) via a 5-membered ring TS to form a cyclic Rh(V) nitrene intermediate is more kinetically favorable, then the facile RE of this Rh(V) species forms the heterocycle product and regenerates Rh(III). Notably, for both reactions, the direct C−N formation from intermediates containing a C(sp^3)−Rh(III)−N(sp^3) unit would be very difficult with barriers over 40 kcal/mol.

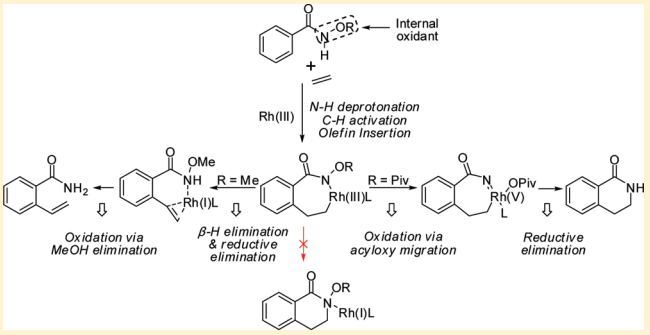

INTRODUCTION

Much effort has been devoted to the conversion of an unactivated C−H bond to a C−C, C−N, or C−O bond in the past decades because this type of research is a powerful way to increase the molecular complexity.[1] One of the major problems in these reactions is to control the regioselectivity of C−H bond cleavage in molecules containing several C−H bonds. Thus, the neighboring heteroatom-directed metal-catalyzed aromatic and olefinic C−H bond functionalizations are widely pursued.[2] However, most of these methods are limited by the drawbacks of high temperature, strong oxidant, and strongly acidic or basic conditions. To avoid these, metal-catalyzed C−H functionalization under external oxidant free condition is highly desirable.[3]

Since the seminal works of Wu and Cui,[4] Hartwig,[5] and Yu,[6] several types of N−O bonds, such as *N*-oxide, *N*-acyloxy, and *N*-methoxy, have been used as the internal oxidants for mild C−H functionalizations.[7] It is recognized that in this strategy the internal oxidants act both as the directing group to facilitate the C−H activation and as the oxidizing agent to regenerate the active catalyst, and improved reactivity, selectivity, and substrate scope are often observed for the reactions with internal oxidants as in comparison with those using external oxidants.[7] Notably, recent independent reports by the groups of Glorius[8a] and Fagnou[8b,c] disclosed an interesting controlling of the reaction pathway by using different internal oxidants (Scheme 1):

Scheme 1. Controlling the Reaction Pathway by Internal Oxidants and Plausible Mechanism

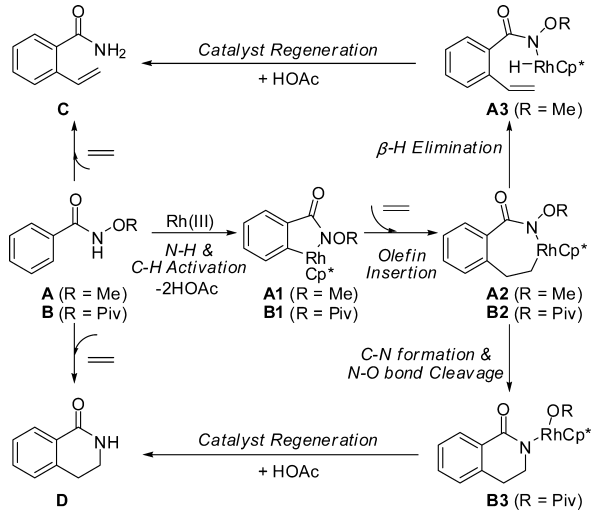

that, in the Rh(III)-catalyzed functionalization of aromatic C−H bond with olefins, the *N*-methoxy benzamide **A** leads exclusively

Received: November 25, 2011
Published: December 27, 2011

   dx.doi.org/10.1021/jo202431q | J. Org. Chem. 2012, 77, 3017−3024

to olefinated product **C**,[8−10] while for the *N*-acyloxy benzamide **B**, the heterocyclic product **D** was obtained from the Rh-catalyzed oxidative cyclization.[8,11,12] Thus, the reaction outcome is dependent on the nature of the internal oxidant.

According to the mechanism shown in Scheme 1, the N−H deprotonation, C−H activation, and olefin insertion steps for **A** to **C** and **B** to **D** transformations are similar, and further reactions from the 7-membered rhodacycles **A2** and **B2** will be controlled by the *N*-OR moiety. The *N*-methoxy-containing intermediate **A2** would undergo *β*-H elimination to generate **A3**, which will lead to the olefination product **C** by reductive elimination (RE) and Rh(I) oxidation. Alternatively, the *N*-acyloxy containing intermediate **B2** may undergo RE and N−O cleavage to form the heterocyclic intermediate **B3**. However, the detailed mechanisms of these reactions have not been investigated, and how the N−O bonds are involved as the internal oxidants to maintain the catalytic cycles and why the olefination and heterocyclization pathways are dependent on the *N*-methoxy and *N*-acyloxy subunits are still unclear. Besides, we assumed that the C−N bond formation in the reaction of **B** may be more complicated than that shown in Scheme 1, as the RE of **B2** (and **A2**) should be difficult in light of the recent computational and experimental works by Yu and co-workers.[13]

Herein, we present a mechanistic study of the above-mentioned reactions by DFT/M06 calculations,[14] with emphasis on understanding the function and divergence of the *N*-methoxy and *N*-acyloxy internal oxidants. Mechanistic insights into the elementary steps in Rh(III)-catalyzed C−H functionalizations with internal oxidants are provided, and the experimentally observed internal oxidant-controlled olefination versus heterocyclization pathways are theoretically rationalized. These results should be useful for future design of new reactions.

COMPUTATIONAL DETAILS

All calculations were carried out by using the Gaussian 09 suite of computational programs.[15] All stationary points along the reaction coordinate were fully optimized at the DFT level using the M06 hybrid functional.[16] This functional was found to be accurate for the thermochemistry and barrier height predictions for systems of both transition metals and main group elements.[16] The standard 6-31G* basis set[17] was applied for all atoms except Rh, which was described by the LANL2DZ basis set and effective core potential implemented.[18] Frequencies were analytically computed at the same level of theory to get the thermodynamic corrections and to confirm whether the structures are minima (no imaginary frequency) or transition states (only one imaginary frequency). Intrinsic reaction coordinate (IRC) calculations[19] were carried out to confirm that all transition state structures connect the proposed reactants and products. The solvation effect was examined by performing single-point self-consistent reaction field (SCRF) calculations[20] based on the polarizable continuum model (PCM) for gas-phase optimized structures. Methanol (ε = 32.61) was used as the solvent, corresponding to the experimental conditions, and the atomic radii used for the PCM calculations were specified using the UFF keyword. Single-point energy calculations were done at the M06 level by using a larger basis set, that SDD for Rh and 6-311+G(d,p) for the rest. All energies reported (ΔG_{MeOH}) are relative single-point energies corrected by the Gibbs free energy correction from frequency calculation and the solvation free energy correction from SCRF calculation.[21]

RESULTS AND DISCUSSION

According to Scheme 1, both substrates **A** and **B** share similar N−H deprotonation, C−H activation, and olefin insertion steps, and different reaction pathways will be observed from the 7-membered rhodacycle intermediates. To evaluate the possible influence of the *N*-OR moiety on the whole reactions, the energetic profiles for the consecutive N−H deprotonation/C−H activation/olefin insertion steps for both substrates **A** and **B** are first presented. Then the mechanisms for the formations of olefination and heterocycle products, respectively, from the *N*-OMe and *N*-OPiv substituted 7-membered rhodacycle intermediates are detailed, and how the *N*-OR moiety functions as the internal oxidant will be discussed.

Consecutive N−H Deprotonation/C−H Activation/Olefin Insertion Sequences for Substrates A and B. In experiments,[8] a catalytic amount of $[Cp^*RhCl_2]_2$ and excess CsOAc additive were used as the precatalytic system. Calculations indicate the formation of $Cp^*Rh(OAc)_2$ from $[Cp^*RhCl_2]_2$ and CsOAc via Rh dimer dissociation and ligand exchange is energetically favorable, with an overall exergonicity of 12.8 kcal/mol. Thus, the acetate-ligated species $Cp^*Rh(OAc)_2$ (**Cat.**) was regarded as the active catalyst in the current systems. The geometry of **Cat.** shows one acetate ligand is bidentate while the other one is monodentate, suggesting that besides the η^5-coordination of the Cp* ligand, the Rh center only has three coordination sites available.

The energetic profiles for the initial steps of substrates **A** and **B** are similar and shown in Figure 1, and the geometric structures for selected intermediates and transition states (TS) in the **B** system are depicted in Figure 2. In the first step, coordination of benzamide substrate (**A** and **B**) to the Rh atom of $Cp^*Rh(OAc)_2$ via the nitrogen site to form **IN1** is energetically unfavorable, as **A-IN1** and **B-IN1** are formed endergonically by 9.9 and 7.9 kcal/mol, respectively. This should be due to the fact that the $Cp^*Rh(OAc)_2$ is relatively electron rich and sterically crowded. Geometries of **A-IN1** and **B-IN1** indicate the Rh···N coordination bond in the latter complex is stronger with a slightly shorter Rh−N distance (2.228 vs 2.335 Å). The deprotonation of the slightly acidic N−H bond of **IN1** by one of the acetate ligand is very easy, and the **A-TS1** and **B-TS1** are only 1−2 kcal/mol above the corresponding complex. One HOAc is released into the reaction medium in this step. The N-metalated intermediate **IN2** is slightly more stable than the corresponding precursor. In both intermediates **A-IN2** and **B-IN2**, the Rh atom almost has no interaction with the ortho C−H bond as implied by long Rh−C2 and Rh−H distances (labeling of the atoms is given in the figures). For example, these two distances in **B-IN2** are 3.512 and 3.098 Å, respectively. In the following step, the C−H activation is realized via **TS2**, in which the resting acetate ligand is the base to deprotonate the ortho aromatic proton and the Rh interacts strongly with both atoms of the breaking C−H bond. The geometry of **B-TS2** shows the O−H, H−C2, Rh−C2, and Rh−H distances are 1.360, 1.298, 2.240, and 2.226 Å, respectively (Figure 2). The activation energies for this step in both **A** and **B** series are around 18 kcal/mol. Such concerted metalation−deprotonation (CMD) process has been well established by recent experimental[22] and computational studies[23] of C−H functionalizations. The possible pathways involving cationic $[Cp^*RhOAc]^+$ catalyst, C−H cleavage prior to the N−H deprotonation, oxygen metalation, and olefinic C−H activation by **Cat.** were ruled out by calculations, as given in the Supporting Information.

By passing the N−H deprotonation and C−H activation steps, 5-membered rhodacycle **IN3** is formed, in which the Rh center is coordinated by the carbonyl oxygen of the generated HOAc of the CMD step. The dissociation of HOAc from **IN3** will generate intermediate **IN4** with a vacant coordination site.

dx.doi.org/10.1021/jo202431q | J. Org. Chem. 2012, 77, 3017−3024

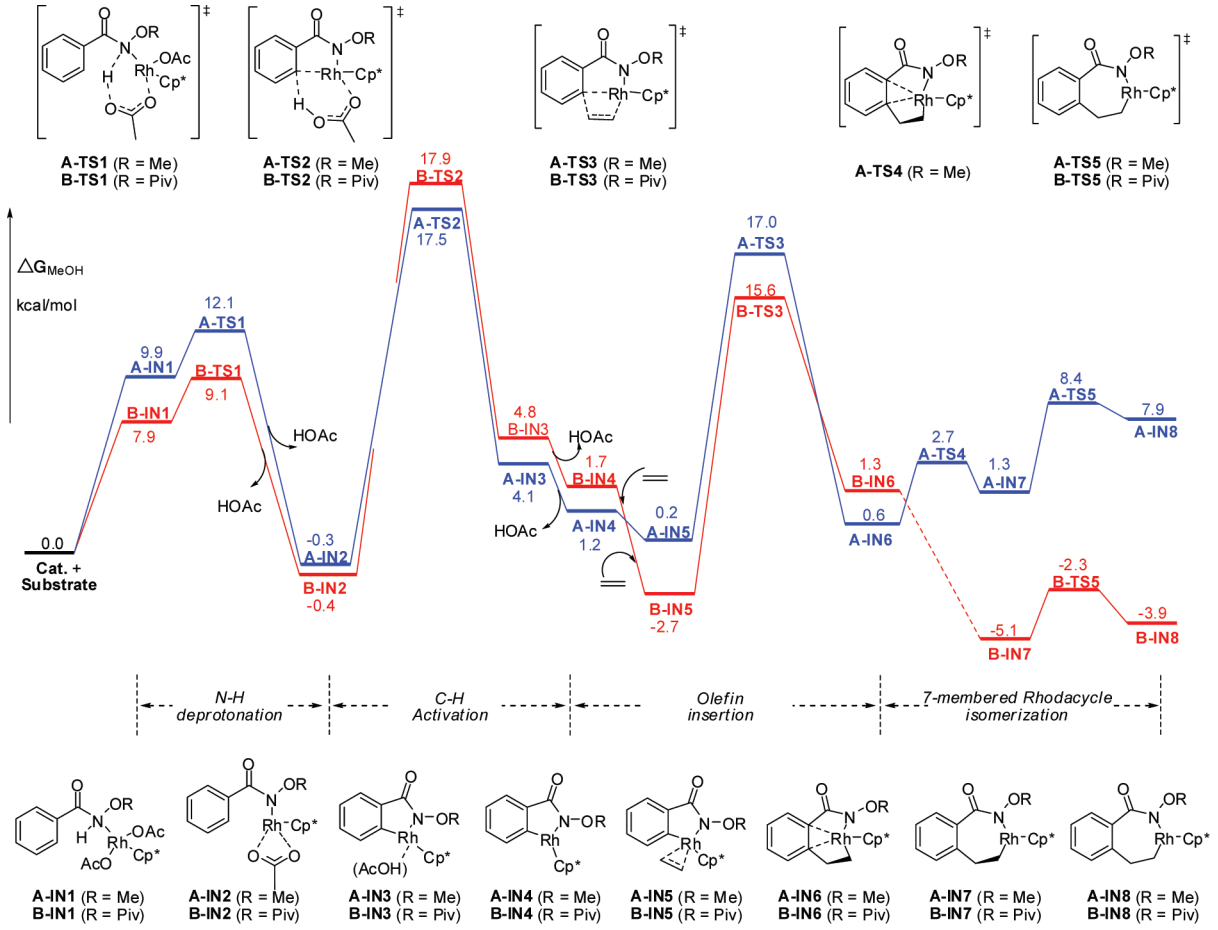

Figure 1. Energy profiles for the consecutive N−H deprotonation/C−H activation/olefin insertion sequences of substrates **A** and **B**.

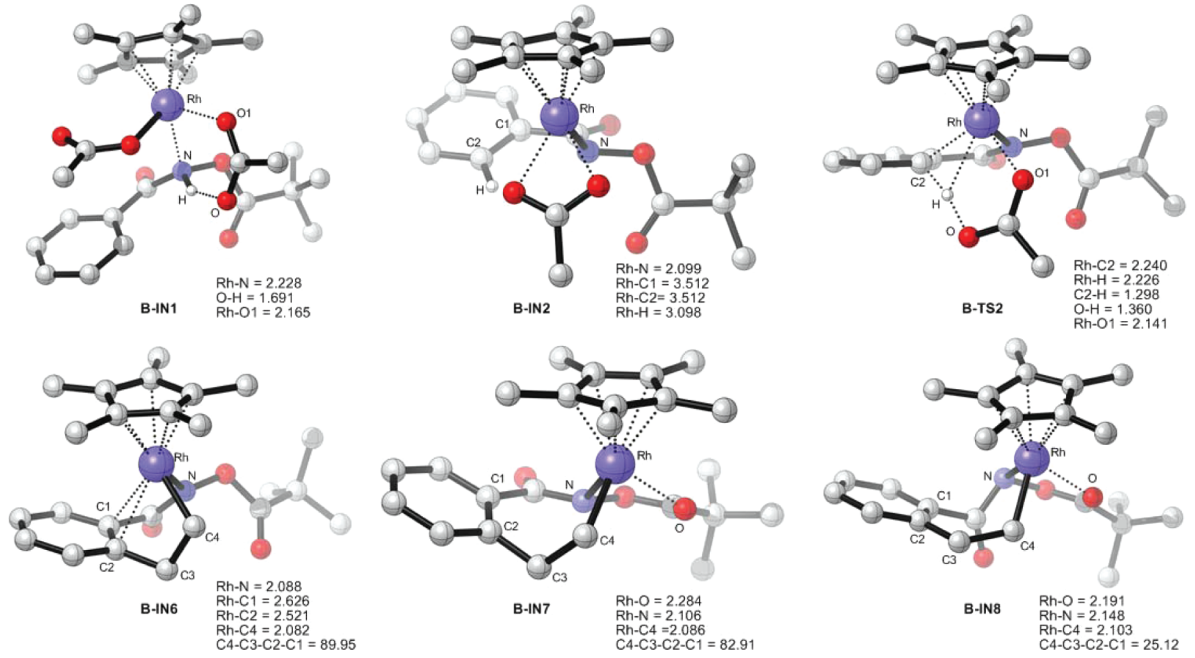

Figure 2. Geometric structures for selected intermediates and TS in the consecutive N−H deprotonation/C−H activation/olefin insertion sequence of substrate **B**; distances and dihedral angles are in angstroms and degree, respectively. All irrelevant hydrogens have been omitted for clarity.

This step is exergonic by about 3 kcal/mol, but the generated intermediate **IN4** is still higher in energy than the isolated catalyst and substrate, indicating the reversibility of the N−H deprotonation/C−H activation processes for both substrates. The coordination of olefin (using ethylene as a model) to **IN4** is exergonic, and **B-IN5** is formed with a relative energy of

dx.doi.org/10.1021/jo202431q | J. Org. Chem. 2012, 77, 3017−3024

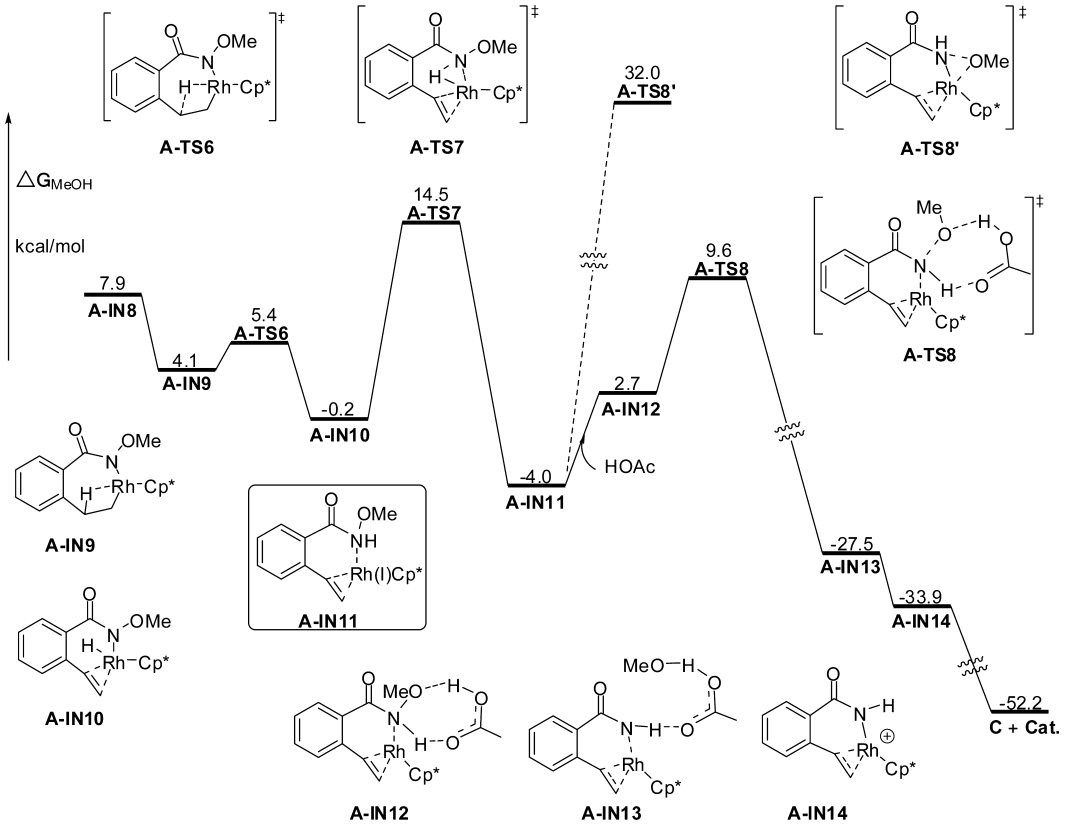

Figure 3. Mechanism for the formation of olefination product **C** from **A-IN8**.

−2.7 kcal/mol while **A-IN5** is 0.2 kcal/mol higher than the starting point. Then the migratory insertion of ethylene into the Rh−C2 bond of **IN5** is realized via **TS3**.[24] The relative energies indicate in the **A** system the olefin insertion TS **A-TS3** (17.0 kcal/mol) is slightly lower than the energy of the C−H cleavage TS **A-TS2** (17.5 kcal/mol), while for the **B** system, the energy gap between **B-IN5** and **B-TS3** is the same as the energy gap between **B-IN2** and **B-TS2** (18.3 kcal/mol). Further results show the activation energies for the C−H cleavage and the olefin insertion steps are the two highest barriers for both reactions of **A** and **B**.

The generated 7-membered rhodacycle from the olefin insertion step is **IN6**. This type of intermediate is puckered as the Rh atom is weakly coordinated with the π electrons between C1 and C2 of the aryl moiety, for example, the Rh−C1 and Rh−C2 distances in **B-IN6** are 2.626 and 2.521 Å, respectively. **IN6** would be transformed into a more flexible intermediate **IN7** by dissociation of the aryl moiety from the Rh center, and this latter intermediate could further isomerize to form **IN8** by rotation of the C−C single bonds. The energies of **TS4** and **TS5** show the interconversions between these 7-membered rhodacycle isomers are very easy. In the **A** series, **A-IN6** is more stable than **A-IN7** and **A-IN8**, probably as results of the coordination unsaturation of the Rh center in the latter two isomers. However, in the **B** series, the **B-IN7** and **B-IN8** are more stable than **B-IN6**, because the *N*-OPiv moiety in these two isomers is a bidentate ligand, stabilizing the intermediates via coordination of the pendant carbonyl oxygen of the acyloxy group to Rh (Figure 2).

Further Reactions from the 7-Membered Rhodacycles of A System. Experimental results by Glorius[8a] and Fagnou[8b,c] found that only the olefination product **C** was obtained from *N*-methoxy-containing substrate **A**, and the β-H elimination from the 7-membered rhodacycle intermediate (Scheme 1) is a key step in this process.[25] Figure 3 shows the detailed mechanism for formation of **C** from **A-IN8** and how the Rh(III) species is regenerated. In this process, **A-IN8** should first isomerize into **A-IN9** by rotation of the C−C single bonds. The latter intermediate is 3.8 kcal/mol more stable, and the geometric structure in Figure 4 indicates the Rh atom has agostic interaction with the C3−H bond, with the Rh−C3 and Rh−H distances being 2.355 and 1.877 Å, respectively. As a result, the C3−H distance is calculated to be 1.174 Å, being obviously elongated than normal C−H bond length.[26,27] Then the β-H elimination occurs via **A-TS6** with an activation barrier of only 1.3 kcal/mol. In this TS the Rh−C3 and Rh−H distances are changed to 2.220 and 1.622 Å, respectively, with the breaking C3−H bond being 1.583 Å. This step leads to a rhodium hydride intermediate[28] **A-IN10** in which the Rh is complexed with the newly formed C−C double bond (Rh−C3 = 2.191 and Rh−C4 = 2.177 Å). From **A-IN10**, the RE is realized via **A-TS7** with an activation barrier of 14.7 kcal/mol, with the breaking Rh−H and forming N−H distances being 1.629 and 1.529 Å respectively, and the Rh−N distance is 2.121 Å, being only elongated by 0.048 Å as in comparison with that distance in **A-IN10**. This step is slightly exergonic with the generated Rh(I) intermediate **A-IN11** being 4.0 kcal/mol lower than the starting material. The Rh(I) center in **A-IN11** is coordinated by both the C3−C4 double bond (Rh−C3 = 2.116 and Rh−C4 = 2.098 Å) and the neutral amide nitrogen (Rh−N = 2.243 Å).

In the following step, oxidation of the Rh(I) species **A-IN11** by the *N*-OMe internal oxidant to regenerate the active Rh(III) catalyst is expected. Figure 3 demonstrates that the intramolecular oxidative addition of the *N*-OMe to Rh(I) to form a

dx.doi.org/10.1021/jo202431q | J. Org. Chem. 2012, 77, 3017−3024

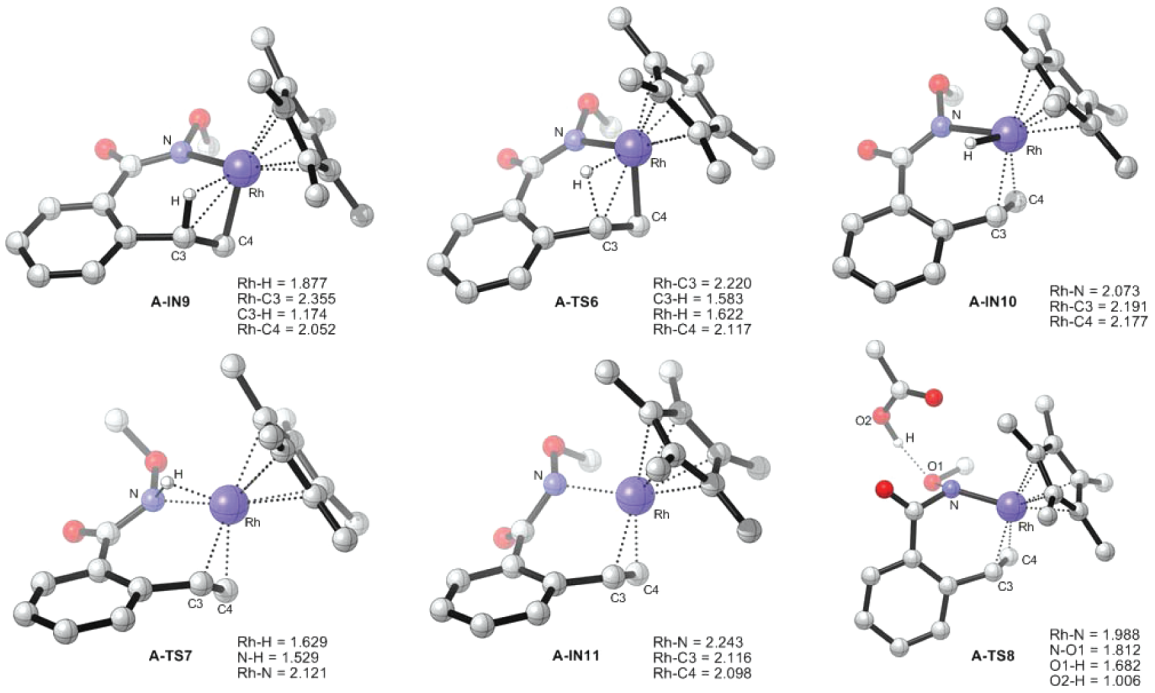

Figure 4. Geometric structures for selected intermediates and TS in the olefination process of substrate **A**; distances are in angstroms. All irrelevant hydrogens have been omitted for clarity.

Rh(III) via TS **A-TS8′**, a formal 1,2-migration of the methoxy from N to Rh, is not possible, as the activation barrier is as high as 36.0 kcal/mol. However, if one HOAc is incorporated to form H-bonding complex **A-IN12**, the elimination of one MeOH could be realized via **A-TS8** with an activation barrier of 13.6 kcal/mol. In this TS, the cleavage of the N−$O1_{methoxy}$ bond and donation of H from HOAc to the OMe moiety occur asynchronously with the O2−H, H−$O1_{methoxy}$, and N−$O1_{methoxy}$ distances being 1.006, 1.682, and 1.812 Å (Figure 4), respectively, and the carbonyl oxygen of the HOAc interacts with the N−H closely (O−H = 1.888 Å, not shown) to form a O···H−N hydrogen bonding. In this way, the Rh(I) intermediate **A-IN11** is transformed irreversibly into Rh(III) intermediate **A-IN13** with an exergonicity of 23.5 kcal/mol. The dissociation of MeOH and acetate from this zwitterionic intermediate to form cationic intermediate **A-IN14** is energetically favorable, and from this intermediate the olefination product **C** could be formed via protonation of the anionic amide ligand by incorporation of a HOAc. The overall exergonicity for formation of **C** from **A** is 52.2 kcal/mol.

The above results show the β-H elimination and RE steps from intermediate **A-IN8** are very easy, and then the Rh(III) is regenerated by MeOH elimination. Scheme 2 depicts the energy for the direct RE of the 7-membered rhodacycle intermediate (**A-IN6**) to form the heterocycle product and the possibilities of the catalyst oxidation occurring before the β-H elimination. These results indicate the RE of **A-IN6** for C−N formation is not possible as the **A-TSa** has a very high relative free energy of 43.8 kcal/mol (eq 1). The very high barrier for C−N formation from **A-IN6** is similar to the previous findings of Yu et al.[13] that the C−C formation from the RE of C(sp^3)−Rh(III)−C(sp^3) unit is much more difficult than that from the RE of C(sp^2)−Rh(III)−C(sp^3) unit.[29] The oxidation of the Rh(III) intermediate into a Rh(V) species by the *N*-OMe functionality has also been ruled out. Likewise, the high energy

Scheme 2

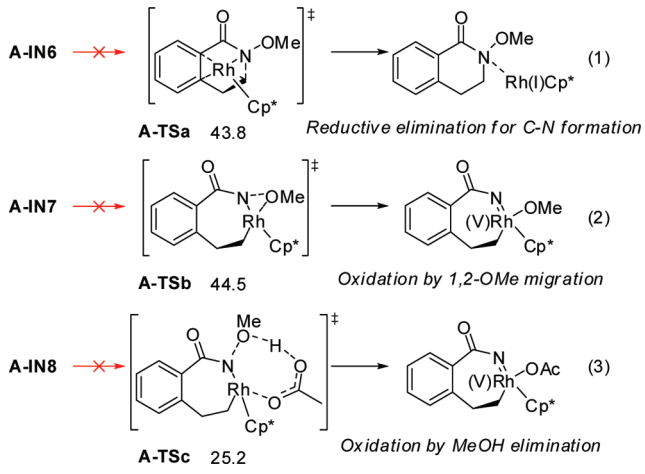

of **A-TS8′** in Figure 3, the intramolecular oxidative addition of the *N*-OMe moiety to Rh(III) of **A-IN7** via a three-center TS **A-TSb** would be very energy demanding (eq 2). The energy for the oxidation of **A-IN8** by MeOH elimination via **A-TSc** could be greatly lowered if one HOAc is involved (eq 3); however, this step is more than 10.0 kcal/mol higher in activation barrier as in comparison with the facile β-H elimination/RE from **A-IN9**. Thus, after the formation of the 7-membered rhodacycle in the **A** system, only the olefination reaction shown in Figure 3 occurs, and the Rh(III)/Rh(I) catalytic cycle is maintained by MeOH elimination from the *N*-OMe moiety.

Mechanism for the C−N Formation from B-IN8. To elucidate how the reaction pathway is controlled by the *N*-OPiv moiety of **B** to give the heterocycle product, the energetic profile for possible reactions from 7-membered rhodacycle **B-IN8** is shown in Figure 5, in which the energies for the

dx.doi.org/10.1021/jo202431q | J. Org. Chem. 2012, 77, 3017−3024

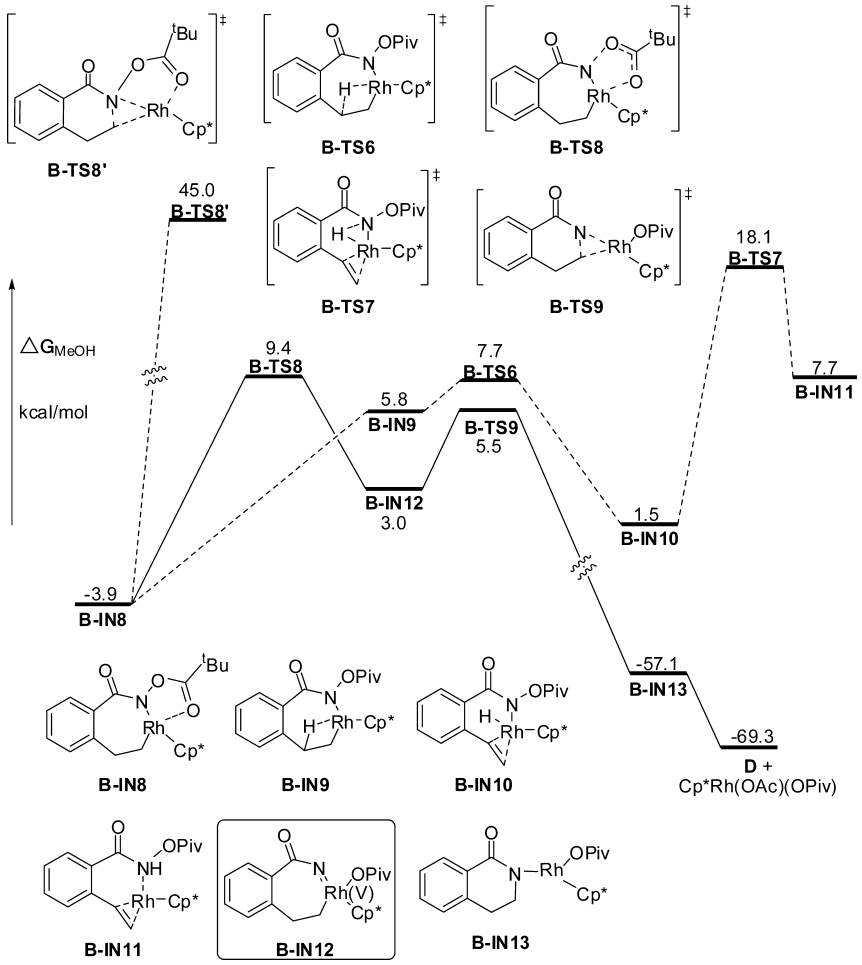

Figure 5. Energy profile for the possible C−N formation and olefination pathways from **B-IN8**.

C−N formation and the possible β-H elimination pathways are compared.

Likewise in Figure 3, if the β-H elimination reaction occurs, **B-IN8** should first isomerize to **B-IN9**, in which the Rh···$O_{Carbonyl}$ coordination in **B-IN8** is replaced by the Rh···C3−H coordination, with the free energy increased by about 9.7 kcal/mol. The β-H elimination occurs via **B-TS6**, which requires a barrier of only 1.9 kcal/mol from **B-IN9**. This step is endergonic by 5.4 kcal/mol from **B-IN8**, and the RE of the generated Rh hydride intermediate **B-IN10** is more difficult than the β-H elimination, with the relative free energy of **B-TS7** being 18.1 kcal/mol. Hence, the activation energy for the formation of the olefination product in the **B** system should be 23.2 kcal/mol, defined by the energy gap between **B-TS7** and **B-IN7** (the global minimum in the **B** system). The key geometric parameters of **B-IN10** (given in the Supporting Information) is very similar to that of **A-IN10**, and we reasoned that the relatively difficult olefination via **B-TS6** and **B-TS7** as in comparison with that of the **A** system could be attributed to two factors: (1) the 7-membered rhodacycle in the **B** system (**B-IN7**) is stabilized with the extra coordination of the carbonyl oxygen of the acyloxy, thus increasing the gap between **B-IN7** and **B-TS7**, and (2) the generated intermediate **B-IN11** is much higher in energy than preceding intermediates, probably due to the steric repulsion between the OPiv moiety and the Cp* ligand. This is in contrast to the thermodynamic preference of that intermediate in the **A** system (**A-IN11**).

We then present the energetic scenario of the C−N formation pathway from **B-IN8**. As expected, the direct RE from **B-IN8** via **B-TS8′** requires a much higher activation barrier than the β-H elimination.[13] This strongly implies there should be other reaction channels that lead to the heterocycle product. Noting that in the reaction of **B** the Rh centers in both **B-IN7** and **B-IN8** are coordinated by the pendant carbonyl oxygen of the *N*-acyloxy moiety, we considered if the migration of acyloxy from N to Rh occurs prior to the C−N formation. The results in Figure 5 show that migration of the OPiv from N to Rh could be realized via a 5-membered ring TS **B-TS8**,[30] in which the breaking N−O distance is 2.506 Å and the forming Rh−O′ distance is 2.082 Å (Figure 6). The activation barrier is 14.5 kcal/mol from **B-IN7**, giving rise to a Rh(V) nitrene intermediate **B-IN12**.[31] The Rh═N distance in this intermediate is 1.871 Å, being much shorter than the Rh−N single bond in **B-IN8** (2.148 Å). As expected, the high oxidation state Rh(V) species **B-IN12** undergoes RE much more easily with a barrier of only 2.5 kcal/mol via **B-TS9** (C4−N = 2.311 Å),[32] leading to **B-IN13** irreversibly. Protonation of the anionic nitrogen site of **B-IN13** by HOAc will lead to the final product **D** and generate the catalytic active Cp*Rh(OAc)(OPiv) concurrently, with an overall exergonicity of 69.3 kcal/mol. Figure 4 shows this acyloxy migration/C−N formation pathway is 8.7 kcal/mol (the energy difference between **B-TS8** and **B-TS7**) more kinetically favorable than the olefination pathway. Thus, a Rh(III)/Rh(V) catalytic cycle is established for the reaction of

dx.doi.org/10.1021/jo202431q | J. Org. Chem. 2012, 77, 3017−3024

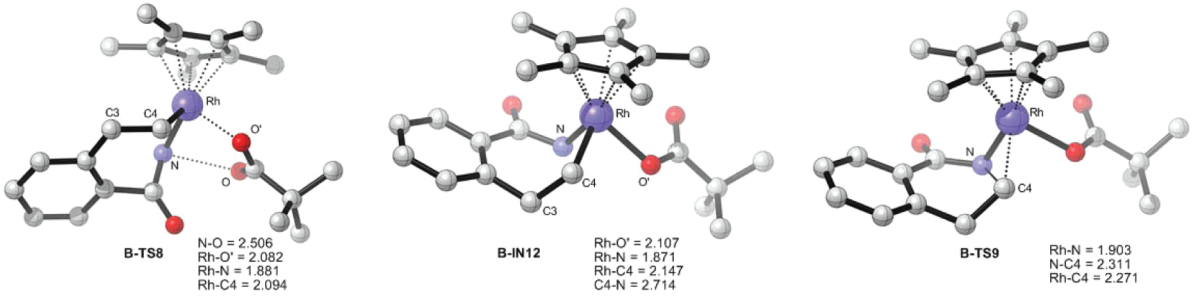

Figure 6. Geometric structures for selected intermediates and TS in the heterocyclization process of substrate **B**; distances are in angstroms. All hydrogens have been omitted for clarity.

N-acyloxy containing substrate **B**, and the C−N formation is facilitated upon the intermediacy of a 7-membered ring Rh(V) nitrene species that resulted from the acyloxy group migration. Otherwise, the C−N bond should be very difficult to form.[33]

CONCLUSION

In summary, the reaction mechanisms of the Rh(III)-catalyzed C−H functionalization of benzamide derivatives with olefin have been studied by DFT calculations. The energetic profiles for the N−H deprotonation/C−H activation (CMD)/olefin insertion sequences of the *N*-OMe- and *N*-OPiv-containing substrates are provided to show how the 7-membered rhodacycles are formed. It is found that in reactions of both substrates the CMD step has the highest activation energy around 18 kcal/mol, while the activation barrier of the olefination insertion step is very close to that of the CMD step. Further reactions from the 7-membered rhodacycles are irreversible, and how the reaction pathways are controlled by different internal oxidants is disclosed. When *N*-OMe is involved, the β-H elimination/RE sequence of the corresponding 7-membered rhodacycle requires an activation barrier of 14.7 kcal/mol, and the formed Rh(I) intermediate could be readily oxidized to the active Rh(III) by MeOH elimination from the reduction of the *N*-OMe moiety in the presence of a HOAc. This process is much more facile than the difficult C−N formation from the cyclic C(sp^3)−Rh(III)−N(sp^3) unit, and leads to the olefination product exclusively. On the other hand, for reactions of the 7-membered rhodacycle containing a *N*-OPiv moiety, which could be stabilized by the coordination of the pendant carbonyl oxygen of the *N*-acyloxy, the activation energy of the olefination through a β-H elimination/RE sequence would be increased to about 23.2 kcal/mol. Instead, the migration of the pivalate from N to Rh via a 5-membered ring TS would be 8.7 kcal/mol more favorable kinetically, leading to a cyclic Rh(V) nitrene intermediate. This Rh(V) species could undergo RE easily to form the C−N bond and to regenerate the Rh(III) catalyst. Thus, the heterocycle product in reaction of *N*-acyloxy benzamide results from an acyloxy migration/C−N formation sequence.

ASSOCIATED CONTENT

Supporting Information

Other possible reaction channels, calculated geometries, energies, and Cartesian coordinates. This material is available free of charge via the Internet at http://pubs.acs.org.

AUTHOR INFORMATION

Corresponding Author

*E-mail: xyz@wzu.edu.cn.

ACKNOWLEDGMENTS

This work is financially supported by the National Natural Science Foundation of China (No. 21002073), Wenzhou Science & Technology Bureau (No. Y20100003), and Wenzhou University (startup funding to Y.X.). Support from the Graduate Innovation Foundation of Wenzhou University to L.X. (No. 3160301010942) and the Xinmiao Talent Program of Zhejiang Province to Q.Z. and L.X. (No. 2010R424043) is acknowledged. All computations were done on the High Performance Computation Platform of Wenzhou University. We thank Guotao Ke of Tianjin University for helping us improve the cover art of this paper.

REFERENCES

(1) For selected reviews, see: (a) Ackermann, L. *Chem. Rev.* **2011**, *111*, 1315. (b) Hartwig, J. F. *Chem. Soc. Rev.* **2011**, *40*, 1992. (c) Gutekunst, W. R.; Baran, P. S. *Chem. Soc. Rev.* **2011**, *40*, 1976. (d) McMurray, L.; O'Hara, F.; Gaunt, M. J. *Chem. Soc. Rev.* **2011**, *40*, 1885. (e) Willis, M. C. *Chem. Rev.* **2010**, *110*, 725. (f) Alberico, D.; Scott, M. E.; Lautens, M. *Chem. Rev.* **2007**, *107*, 174. (g) Beck, E. M.; Gaunt, M. J. *Top. Curr. Chem.* **2010**, *292*, 85. (h) Sun, C.-L.; Li, B.-J.; Shi, Z.-J. *Chem. Commun.* **2010**, *46*, 677. (i) Davies, H. M. L.; Du Bois, J.; Yu, J.-Q. *Chem. Soc. Rev.* **2011**, *40*, 1855. (j) Sames, D.; Godula, K. *Science* **2006**, *312*, 67. (k) Ackermann, L.; Vicente, R; Kapdi, A. *Angew. Chem., Int. Ed.* **2009**, *48*, 9792. (l) Chiusoli, G. P.; Catellani, M.; Costa, M.; Motti, E.; Ca', N. D.; Maestri, G. *Coord. Chem. Rev.* **2010**, *254*, 456.

(2) For reviews, see: (a) Wencel-Delord, J.; Dröge, T.; Liu, F.; Glorius, F. *Chem. Soc. Rev.* **2011**, *40*, 4740. (b) Colby, D. A.; Bergman, R. G.; Ellman, J. A. *Chem. Rev.* **2010**, *110*, 624. (c) Lyons, T. W.; Sanford, M. S. *Chem. Rev.* **2010**, *110*, 1147. (c) Kakiuchi, F.; Murai, S. *Acc. Chem. Res.* **2002**, *35*, 826.

(3) (a) Ureshino, T.; Yoshida, T.; Kuninobu, Y.; Takai, K. *J. Am. Chem. Soc.* **2010**, *132*, 14324. (b) Simmons, E. M.; Hartwig, J. F. *J. Am. Chem. Soc.* **2010**, *132*, 17092. (c) Tsukada, N.; Hartwig, J. F. *J. Am. Chem. Soc.* **2005**, *127*, 5022.

(4) Wu, J.; Cui, X.; Chen, L.; Jiang, G.; Wu, Y. *J. Am. Chem. Soc.* **2009**, *131*, 13888.

(5) Tan, Y.; Hartwig, J. F. *J. Am. Chem. Soc.* **2010**, *132*, 3676.

(6) Ng, K.-H.; Chan, A. S. C.; Yu, W.-Y. *J. Am. Chem. Soc.* **2010**, *132*, 12862.

(7) Patureau, F. W.; Glorius, F. *Angew. Chem., Int. Ed.* **2011**, *50*, 1977.

(8) (a) Rakshit, S.; Grohmann, C.; Besset, T.; Glorius, F. *J. Am. Chem. Soc.* **2011**, *133*, 2350. (b) Guimond, N.; Gorelsky, S. I.; Fagnou, K. *J. Am. Chem. Soc.* **2011**, *133*, 6449. (c) Guimond, N.; Gouliaras, C.; Fagnou, K. *J. Am. Chem. Soc.* **2010**, *132*, 6908.

(9) Willwacher, J.; Rakshit, S.; Glorius, F. *Org. Biomol. Chem.* **2011**, *9*, 4736.

(10) For recent examples of Rh-catalyzed olefinations in the presence of external oxidants, see: (a) Patureau, F. W.; Besset, T.; Glorius, F. *Angew. Chem., Int. Ed.* **2011**, *50*, 1064. (b) Gong, T.-J.; Xiao, B.; Liu, Z.-J.; Wang, J.; Xu, J.; Luo, D.-F.; Fu, Y.; Liu, L. *Org. Lett.* **2011**, *13*,

3235. (c) Patureau, F. W.; Glorius, F. *J. Am. Chem. Soc.* **2010**, *132*, 9982. (d) Umeda, N.; Hirano, K.; Satoh, T.; Miura, M. *J. Org. Chem.* **2009**, *74*, 7094. (e) Mochida, S.; Hirano, K.; Satoh, T.; Miura, M. *Org. Lett.* **2010**, *12*, 5776. (f) Park, S. H.; Kim, J. Y.; Chang, S. *Org. Lett.* **2011**, *13*, 2372. (g) Zou, G.; Wang, Z.; Zhu, J.; Tang, J. *Chem. Commun.* **2003**, 2438.

(11) (a) Li, B.; Feng, H.; Xu, S.; Wang, B. *Chem.—Eur. J.* **2011**, *17*, 12573. (b) Too, P. C.; Chua, S. H.; Wong, S. H.; Chiba, S. *J. Org. Chem.* **2011**, *76*, 6159. (c) Too, P. C.; Wang, Y.-F.; Chiba, S. *Org. Lett.* **2010**, *12*, 5688.

(12) For recent examples of Rh-catalyzed C-N formations in the presence of external oxidants, see: (a) Parthasarathy, K.; Cheng, C.-H. *J. Org. Chem.* **2009**, *74*, 9359. (b) Wei, X.; Zhao, M.; Du, Z.; Li, X. *Org. Lett.* **2011**, *13*, 4636. (c) Song, G.; Gong, X.; Li, X. *J. Org. Chem.* **2011**, *76*, 7583. (d) Hyster, T. K.; Rovis, T. *J. Am. Chem. Soc.* **2010**, *132*, 10565. (e) Wang, F.; Song, G.; Li, X. *Org. Lett.* **2010**, *12*, 5430. (f) Wang, Y.-F.; Toh, K. K.; Lee, J.-Y.; Chiba, S. *Angew. Chem., Int. Ed.* **2011**, *50*, 5927. (g) Guimond, N.; Fagnou, K. *J. Am. Chem. Soc.* **2009**, *131*, 12050. (h) Ueura, K.; Satoh, T.; Miura, M. *Org. Lett.* **2007**, *9*, 1407.

(13) (a) Wang, Y.; Wang, J.; Su, J.; Huang, F.; Jiao, L.; Liang, Y.; Yang, D.; Zhang, S.; Wender, P. A.; Yu, Z.-X. *J. Am. Chem. Soc.* **2007**, *129*, 10060. (b) Yu, Z.-X.; Wender, P. A.; Houk, K. N. *J. Am. Chem. Soc.* **2004**, *126*, 9154. (c) Ozawa, F.; Mori, T. *Organometallics* **2003**, *22*, 3593.

(14) For selected recent examples of DFT study of Rh catalysis, see: (a) Jiao, L.; Lin, M.; Yu, Z.-X. *J. Am. Chem. Soc.* **2011**, *133*, 447. (b) Shi, F.-Q. *Org. Lett.* **2011**, *13*, 736. (c) Evans, M. E.; Burke, C. L.; Yaibuathes, S.; Clot, E.; Eisenstein, O.; Jones, W. D. *J. Am. Chem. Soc.* **2009**, *131*, 13464. (d) Nova, A.; Ujaque, G.; Albéniz, A. C.; Espinet, P. *Chem.—Eur. J.* **2008**, *14*, 3323.

(15) Gaussian 09, Revision A.02, Frisch, M. J. et al., Gaussian, Inc., Wallingford CT, 2009.

(16) (a) Zhao, Y.; Truhlar, D. G. *Acc. Chem. Res.* **2008**, *41*, 157. (b) Zhao, Y.; Truhlar, D. G. *Theor. Chem. Acc.* **2008**, *120*, 215. (c) Truhlar, D. G. *J. Am. Chem. Soc.* **2008**, *130*, 16824. (d) Zhao, Y.; Truhlar, D. G. *J. Chem. Theory Comput.* **2009**, *5*, 324.

(17) (a) Hehre, W. J.; Ditchfield, R.; Pople, J. A. *J. Chem. Phys.* **1972**, *56*, 2257. (b) Hariharan, P. C.; Pople, J. A. *Theor. Chim. Acta* **1973**, *28*, 213.

(18) (a) Hay, P. J.; Wadt, W. R. *J. Chem. Phys.* **1985**, *82*, 270. (b) Wadt, W. R.; Hay, P. J. *J. Chem. Phys.* **1985**, *82*, 284. (c) Hay, P. J.; Wadt, W. R. *J. Chem. Phys.* **1985**, *82*, 299.

(19) (a) Gonzalez, C.; Schlegel, H. B. *J. Chem. Phys.* **1989**, *90*, 2154. (b) Gonzalez, C.; Schlegel, H. B. *J. Phys. Chem.* **1990**, *94*, 5523.

(20) Tomasi, J.; Persico, M. *Chem. Rev.* **1994**, *94*, 2027.

(21) We have also studied the reactions by using the B3PW91/6-31G*(LANL2DZ) method. The results support the same conclusions, but higher activation barriers are predicted. See the Supporting Information for details.

(22) (a) Li, L.; Brennessel, W. W.; Jones, W. D. *Organometallics* **2009**, *28*, 3492. (b) Davies, D. L.; Al-Duaij, O.; Fawcett, J.; Giardiello, M.; Hilton, S. T.; Russell, D. R. *Dalton Trans.* **2003**, 4132.

(23) (a) Davies, D. L.; Donald, S. M. A.; Macgregor, S. A. *J. Am. Chem. Soc.* **2005**, *127*, 13754. (b) Lafrance, M.; Fagnou, K. *J. Am. Chem. Soc.* **2006**, *128*, 16496. (c) Lafrance, M.; Rowley, C. N.; Woo, T. K.; Fagnou, K. *J. Am. Chem. Soc.* **2006**, *128*, 8754. (d) García-Cuadrado, D.; Braga, A. A. C.; Maseras, F.; Echavarren, A. M. *J. Am. Chem. Soc.* **2006**, *128*, 1066. (e) Garcia-Cuadrado, D.; de Mendoza, P.; Braga, A. A. C.; Maseras, F.; Echavarren, A. M. *J. Am. Chem. Soc.* **2007**, *129*, 6880. (f) Gorelsky, S. I.; Lapointe, D.; Fagnou, K. *J. Am. Chem. Soc.* **2008**, *130*, 10848. (g) Boutadla, Y.; Davies, D. L.; Macgregor, S. A.; Poblador-Bahamonde, A. I. *Dalton Trans.* **2009**, 5820. (h) Lapointe, D.; Fagnou, K. *Chem. Lett.* **2010**, *39*, 1118. (i) Sun, H.-Y.; Gorelsky, S. I.; Stuart, D. R.; Campeau, L.-C.; Fagnou, K. *J. Org. Chem.* **2010**, *75*, 8180. (j) Anand, M.; Sunoj, R. B. *Org. Lett.* **2011**, *13*, 4802. (k) Tang, S.-Y.; Guo, Q.-X.; Fu, Y. *Chem.—Eur. J.* **2011**, *17*, 13866. (l) Chen, B.; Hou, X.-L.; Li, Y.-X.; Wu, Y.-D. *J. Am. Chem. Soc.* **2011**, *133*, 7668. (m) Santoro, S.; Liao, R.-Z.; Himo, F. *J. Org. Chem.* **2011**, *76*, 9246. (n) Zhang, S.; Shi, L.; Ding, Y. *J. Am. Chem. Soc.* **2011**, *133*, 20218.

(24) Li, L.; Jiao, Y.; Brennessel, W. W.; Jones, W. D. *Organometallics* **2010**, *29*, 4593.

(25) (a) Li, Z.; Fu, Y.; Zhang, S. L.; Guo, Q.-X.; Liu, L. *Chem. Asian J.* **2010**, *5*, 1475. (b) Wang, C.; Fu, Y.; Li, Z.; Guo, Q.-X. *Chin. J. Chem.* **2008**, *26*, 358. (c) Finger, M.; Reek, J. N. H.; de Bruin, B. *Organometallics* **2011**, *30*, 1094. (d) Theofanis, P. L.; Goddard, W. A. *Organometallics* **2011**, *30*, 4941.

(26) McMurry, J. *Organic Chemistry*, 5th ed.; Thomson Learning: Pacific Grove, 1999.

(27) NBO analysis of **A-IN9** indicates the bond orders for C3-H, C3-Rh, and Rh-H are 0.71, 0.16, and 0.14, respectively.

(28) (a) Ke, Z.; Abe, S.; Ueno, T.; Morokuma, K. *J. Am. Chem. Soc.* **2011**, *133*, 7926. (b) Watkins, A. L.; Landis, C. R. *J. Am. Chem. Soc.* **2010**, *132*, 10306.

(29) The alkenyl analogue of **A-IN6** (**E**), which could result from the insertion of an alkyne into the Rh−C2 bond of **A-IN4** and has a C(sp^2)−Rh(III)−N(sp^3) subunit, undergoes the RE (**E-TS**) more easily with an activation barrier of about 20.0 kcal/mol. This is consistent with the discovery of Yu et al.[13a]

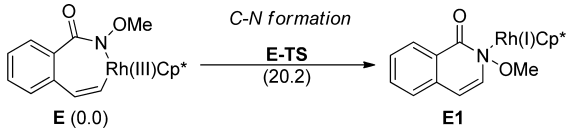

(30) Such 1,2-acyloxy migrations via the 5-membered TS are known; for a recent example, see: Gary, J. B.; Sanford, M. S. *Organometallics* **2011**, *30*, 6143.

(31) For examples involving Rh(V) species, see: (a) Brayshaw, S. K.; Sceats, E. L.; Green, J. C.; Weller, A. S. *Proc. Natl. Acad. Sci. U.S.A.* **2007**, *104*, 6921. (b) McBee, J. L.; Escalada, J.; Tilley, T. D. *J. Am. Chem. Soc.* **2009**, *131*, 12703. (c) Vyboishchikov, S. F.; Nikonov, G. I. *Organometallics* **2007**, *26*, 4160.

(32) In the Rh(III)-mediated C−H activation for isoquinolinium salt synthesis, Jones et al. proposed the Rh(IV) species should be formed for reductive C−N formation; see: Li, L.; Brennessel, W. W.; Jones, W. D. *J. Am. Chem. Soc.* **2008**, *130*, 12414.

(33) The alkenyl analogue of **B-IN8** (**F**) could form the C-N bond via a stepwise RE/N−O cleavage mechanism;[8b,29] however, the formation of a Rh(V) species (**F3**) via a first acyloxy migration from N to Rh (**F-TS3**) would be much more facile.